

Density and viscosity calculation using ultrasonic wave propagation

by

Olivier Schuringa

to obtain the degree of Bachelor of Science
at the Delft University of Technology,
to be defended publicly on Friday December 8, 2017 at 10:30 AM.

Student number: 4367995
Project duration: September 18, 2017 – December 8, 2017
Thesis committee: S. Mastromarino, TU Delft, supervisor
Dr. ir. M. Rohde, TU Delft
Prof. dr. ir. J. L. Kloosterman, TU Delft

An electronic version of this thesis is available at <http://repository.tudelft.nl/>.



Abstract

Within the Generation-IV reactors, the Molten Salt Fast Reactor (MSFR) offers several advantages regarding sustainability, economic competitiveness, proliferation resistance and especially safety. The SAMOFAR (Safety Assessment of the Molten Salt Fast Reactor) project has the main goal of: delivering a breakthrough in reactor safety and nuclear waste management. For safety concerns it is necessary to know the fluid behaviour in the reactor. Density and viscosity are essential to determine the neutronic behaviour of the fuel and to predict the flow and turbulent heat transfer through the reactor circuit. Density and viscosity cannot be measured with a standard viscometer due to high temperature, radioactivity and corrosiveness of the molten salt. Therefore it is necessary to develop a new type of viscometer. In this research a non-destructive ultrasonic instrument is used to measure density and viscosity. In order to avoid contact of the transducer, that transmits the waves, with the fluid, a waveguide is used. In this research, ultrasonic waves are guided through a copper rod to measure properties of glycerol. Copper and glycerol are chosen as reference materials for their availability and their acoustic and physical properties similar to the ones of the fuel and the waveguide material usable for it. The ultrasonic waves and the simulated set up were created with the commercial software, COMSOL. The set up was optimised in order to measure acoustic properties, such as speed of sound, reflection coefficient and attenuation, and physical properties, such as the density and viscosity, of glycerol. The obtained results are respectively, 1939 m/s for the speed of sound which deviates 0.9% from the actual value, 0.882 for the reflection coefficient between copper and glycerol which deviates 0.99%, 1332 kg/m³ for the density which deviates 5.73%, 17.08 1/m for the attenuation coefficient with a deviation of 52.33% and 1.58 Pa s for the viscosity with a deviation from the theoretical value of 66.36%. The deviation of viscosity is primarily caused by the attenuation coefficient. The reason for such deviation is that the received wave from glycerol and the trailing echoes come back at the receiver at approximately the same time interval. Therefore no clear distinction can be made between desired signal and noise. To improve the determination of the density and viscosity, it is necessary to eliminate the trailing echoes as much as possible. Also, a minimum of two immersion depths has to be chosen at which the trailing echoes are minimised. It is important to collect as much data as possible for the calculation of the attenuation coefficient, thus more simulations have to be done. Lastly, instead of using acoustic waves in a waveguide it is possible to use surface waves for the determination of density and viscosity. This should be investigated in further research. If the determination of the density and viscosity are optimised, eventually predictions can be made of critical information for the MSFR. This will contribute to the final goal of this project delivering experimental proof of the safety and sustainability features of the MSFR.

Contents

1	Introduction	1
1.1	The Molten Salt Fast Reactor	1
1.2	Thermodynamic properties and ultrasonic wave measuring	2
1.3	Previous research	3
1.4	Research goals	3
2	Theory	5
2.1	The acoustic wave equation	5
2.2	The solid-liquid interface	6
2.3	Thermodynamic property calculations	7
2.4	Surface acoustic waves	8
2.5	Dispersion	9
3	Experimental and simulation method	11
3.1	The experimental set up	11
3.2	The simulation method	13
3.2.1	The model environment	13
3.2.2	Create geometric objects	13
3.2.3	Specify material properties	13
3.2.4	Define physics boundary conditions	14
3.2.5	Create the mesh	14
3.2.6	Run the simulation and post-process the results	15
3.3	Experimental method	15
4	Results and discussion	16
4.1	2D model with immersion	16
4.2	2D model without immersion	18
4.3	Measurement method optimisation	20
4.4	2D model without immersion; smaller waveguide	22
4.5	2D model without immersion; smaller tapered waveguide	24
4.5.1	Density calculation	24
4.5.2	Attenuation measurement and viscosity calculation	26
5	Conclusion and recommendation	28
A	Parameters	29
	Bibliography	31

Chapter 1

Introduction

The ever increasing energy demand is an important issue for the world in this new millennium. Even if coal, oil and gas are a cheap and immediate energy source, they will eventually finish and can have a negative effect on the climate of Earth. Wind and solar energy are good substitutions for reducing the carbon emission but cannot produce the same amount of energy as the fossil fuels. Although nuclear energy can yield an enormous amount of energy, is reliable, sustainable and economical competitive, controversial arguments exist because of the safety concerns and historic accidents, for instance Chernobyl (1986) and Fukushima (2011).

In 2000, during the Generation IV International Forum, six new types of nuclear reactors were proposed [1]. These new generation of reactors excel in the area of safety. The Molten Salt Fast Reactor (MSFR) is one of this new generation reactors.

SAMOFAR (Safety Assessment of the Molten Salt Fast Reactor) is a European research project with the goal to make nuclear energy truly safe, sustainable and create new technology for managing nuclear waste [2]. This research is part of this project.

1.1 The Molten Salt Fast Reactor

The most present-day reactors are from the third generation which work with solid fuel which initiate a controlled nuclear chain reaction inside the core of the reactor. The reaction creates heat that is absorbed by a coolant, carried away from the reactor and used to generate steam for electricity.

The main difference between this type of reactors and the MSFR is the use of a liquid fuel instead of a solid fuel. The fuel consists of a molten salt mixture in which there are fertile and fissile elements [3]. The fission occurs within the fuel salt inside the core of the reactor. Afterwards, the liquid will flow to a heat exchanger where the heat is transferred to a secondary liquid salt which eventually leads to an electricity generator. In figure 1.1 a schematic representation of a MSFR is shown. There are several advantages in using a liquid fuel: firstly it serves the dual function of fuel and heat transfer medium, second, a nuclear meltdown is insignificant, third, the reactor works at normal atmosphere pressure making an explosion impossible, fourth, the molten fuel salt has a high boiling point, which means that the pressure in the reactor tank will be low reducing the risk of a rupture, fifth, in accidental conditions a security measure will make sure that the fluid will be drained in designated storage tanks and lastly, because the fuel is a liquid, it expands when heated and this slows the rate of nuclear reaction [4].

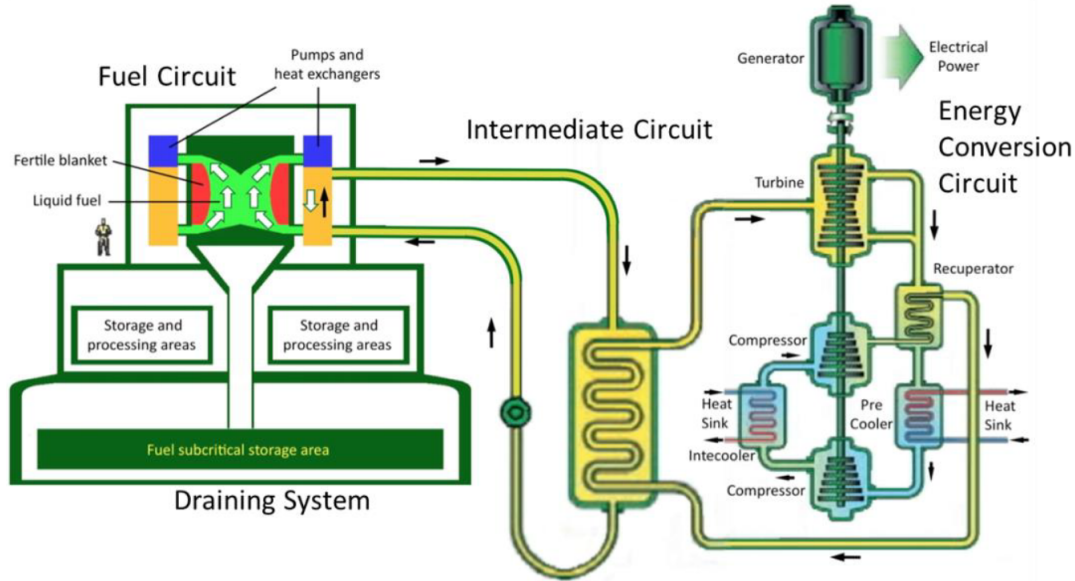


Figure 1.1: Schematic representation of an MSFR [5]

1.2 Thermodynamic properties and ultrasonic wave measuring

A fundamental step for the design of the MSFR is the selection of the exact composition of the fuel. Criteria to take in consideration are: a low melting point, low absorption cross-section, low radiation-induced radioactivity and high chemical stability. Eventually, all these criteria have to be incorporated in the final composition of the salt. Considering the liquid state of the fuel, it is important to know certain properties of this salt in order to predict its behaviour inside the reactor. These thermodynamic properties are density, viscosity, specific heat capacity and thermal conductivity. The density is important for the determination of the behaviour of the neutrons in the fuel and the viscosity is critical for the prediction of the flow and the heat transfer in the reactor circuit. The specific heat capacity shows how much energy can be stored in a volume, thus a higher specific heat capacity corresponds to a smaller storage tank and the large thermal conductivity is desirable to create large heat transfer. In this research the focus is on the development of a measurement method of viscosity and density of the molten salt fuel. These two properties are critical to know but are impossible to measure with current devices because of the temperature, the corrosiveness and the radioactivity of the molten salt.

An alternative way of measuring these properties is by ultrasonic non-destructing testing. This technique works with very short ultrasonic wave pulses and high frequencies (MHz). The great advantage of this technique for the determination of thermodynamic properties is the possibility to measure the density and the viscosity at the same time. The ultrasonic waves are created by a piezo-electric transducer and sent through the fluid. This piezo-electric transducer cannot be placed directly in the fluid because of the high temperature that would exceed its Curie temperature [6], which implies that the transducer becomes depolarised and does not work anymore. Therefore a waveguide is used between the transducer and the fluid to avoid the direct contact with the radioactive salt. In this research the viscosity measurement technique is based on the attenuation of the amplitude of the transmitted wave in the fluid.

1.3 Previous research

While in a fluid only longitudinal waves can exist due to the lack of its shear strength, the ultrasonic waves in the solid consist of longitudinal and shear waves. At the boundaries of the solid the longitudinal and shear waves can be mode converted into each other. The converted waves are called trailing or spurious echoes. These are measured by the receiver. Their contribution to the measured signal has to be minimised in order to measure the viscosity accurately. According to previous research [7] waves inside the buffer rod can be divided in three types which cause the trailing echoes: head waves, longitudinal wave fronts and edge waves, see figure 1.2. The contribution of these trailing echoes depend on the incident angle they made with the free boundary of the rod. Ihara et al. [8] recommend that tapering or cladding of the rod could be the way to minimise the creation of these echoes.

In other previous research [9] an optimal angle for the tapering of a specific rod was evaluated. This was done for a copper rod with a length of 83 mm and a width of 10 mm. These dimensions were chosen to replicate experimental results. The material copper was used because its properties are similar to real material used in the experiment. The optimal angle was determined at 1.25° . A comparison between a wave propagated in a straight rod and in a tapered rod can be done. For example, in figure 1.3 a pulse measurement is shown with a 0° tapering angle. In figure 1.4 a pulse measurement is shown with a 1.25° tapering angle.

1.4 Research goals

This research is part of the SAMOFAR project. The final goal of this project is to deliver experimental proof of the safety and sustainability features of the MSFR. To accomplish this it is imperative to know the fluid behaviour in the reactor and the fluid dynamics such as if the flow is laminar or turbulent. To determine this, density and viscosity are essential. As stated previously, these properties cannot be measured with a standard viscometer due to high the temperature, radioactivity and corrosiveness of the molten salt. Therefore, it is necessary to develop a new type of viscometer using ultrasonic waves to measure the density and viscosity of the fuel. In order to achieve this, the behaviour of the waves at the interface of the buffer rod with the liquid is investigated with the program COMSOL Multiphysics [10]. Measurements and calculations in 2D are done to determine the reflection coefficients of the fluid which is needed to calculate the density, the speed of sound in the fluid and the attenuation coefficient to calculate the viscosity. The results of the measurements are used to optimise the set up of the measuring device.

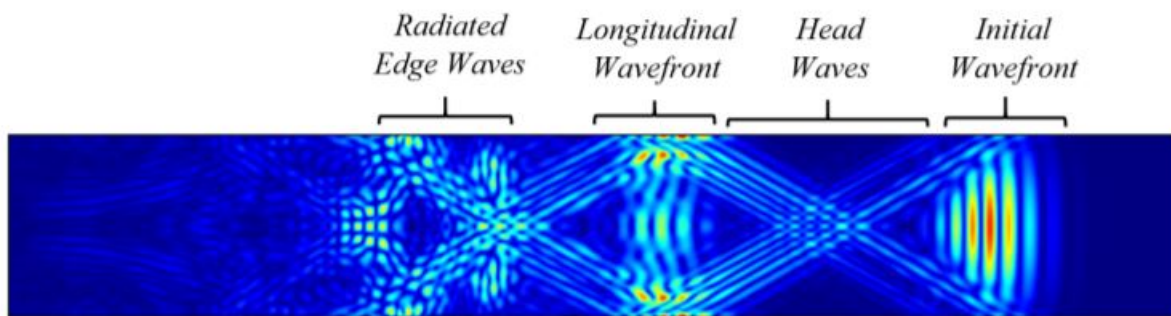


Figure 1.2: Different waves inside the buffer rod [7].

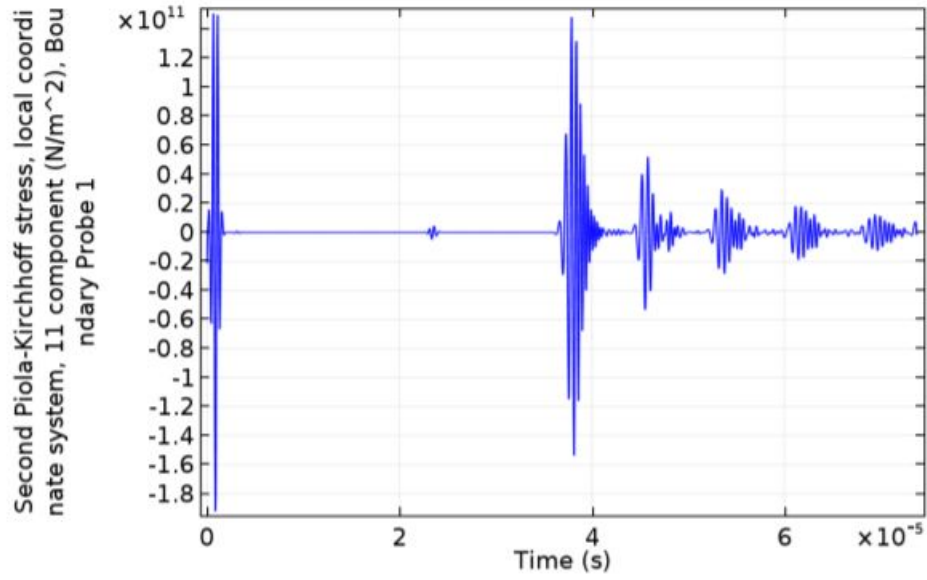


Figure 1.3: Signal of an ultrasonic wave propagating in an untapered rod with length of 83 mm and width of 10 mm [9].

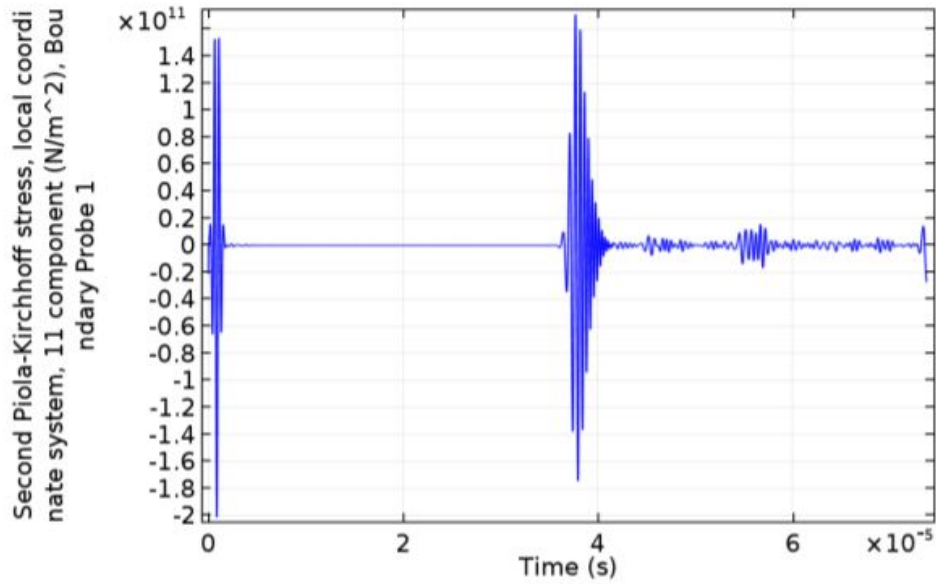


Figure 1.4: Signal of an ultrasonic wave propagating in a tapered rod with length of 83 mm and width of 10 mm; tapering angle of 1.25° [9].

Chapter 2

Theory

In this chapter the theoretical background of the research is covered. The theory of acoustic waves, the reflection coefficient and the calculation method of the thermodynamic properties are discussed. In order to evaluate the results of measurements the topics Surface Acoustic Waves (SAW) and dispersion are treated in this section as well.

2.1 The acoustic wave equation

An acoustic wave is a longitudinal wave which propagates in the same direction as its medium displacement. Acoustic waves are created by a disturbance in a medium causing a pressure difference in the medium. This wave can be created using a piezo-electric transducer where the crest is the maximum value and the trough the minimum value. The wave equation of a 3D acoustic wave is given by [11]

$$\nabla^2 \vec{p}(t) - \frac{1}{c^2} \frac{\partial^2 \vec{p}(t)}{\partial t^2} = 0, \quad (2.1)$$

where $p(x, y, z, t) = \vec{p}(t)$ is the pressure vector and c is the speed of sound of a wave in a specific medium and defined as

$$c^2 = \frac{1}{\rho\kappa}, \quad (2.2)$$

where ρ is the density and κ is the compressibility of the medium. Equation 2.1 is derived from the combination of Newton's equation of motion and Hooke's law of deformation, but is only valid for inviscid fluids. The wave equation for viscous fluids has the difference that in Newton's equation of motion the viscosity of the medium has been incorporated. This equation is given by [7],

$$\nabla^2 \vec{p}(t) - \frac{1}{c^2} \left(\frac{\partial^2 \vec{p}(t)}{\partial t^2} + \frac{4\mu}{3\rho} \frac{\partial \nabla^2 \vec{p}(t)}{\partial t} \right) = 0 \quad (2.3)$$

In order to derive the thermodynamic properties of the fluid the attenuation coefficient of the fluid should be considered. To find this coefficient the general solution for a plane pressure wave is used [11]

$$p(x, t) = p_0 e^{\pm i(kx - \omega t)}, \quad (2.4)$$

where ω is the angular frequency, x is the direction of propagation and $k = \frac{\omega}{c}$ is the wave number. Equation 2.3 can be solved using the expression of the plane wave. This changes the dispersion relation, $k = \frac{\omega}{c}$, from an inviscid fluid to

$$k = \pm \frac{\omega}{c} \left(1 + i\omega \frac{4}{3} \frac{\mu}{\rho c^2} \right)^{-1/2} = \pm(\beta - i\alpha), \quad (2.5)$$

where $c = \frac{\omega}{\beta}$ is the phase velocity and α the attenuation coefficient. This attenuation coefficient is crucial for the calculation of the thermodynamic property of a viscous fluid in this research. It can be derived by using a the Taylor expansion theorem and therefore becomes

$$\alpha = \frac{2\omega^2\mu}{3\rho c^3}, \quad (2.6)$$

where all the parameters are the properties of the fluid.

2.2 The solid-liquid interface

When a wave propagates from a domain to another one a part of the wave reflects from the interface and another part is transmitted in the other domain. In this research we are concerned with pressure waves propagating from a solid to a liquid. At the solid-liquid interface there is a geometrical boundary conditions which holds for all waves. It states that the wave numbers of the incoming (k_1), reflected (k'_1) and transmitted (k_2) waves at the interface between two domains with different properties must be equal to each other [11].

$$k_1 = k'_1 = k_2 \quad (2.7)$$

In this research, the acoustic waves are propagated perpendicularly to the interface. If the incoming wave makes an angle of θ_1 with the normal and the transmitted wave makes an angle of θ_2 with the normal, it can be described as

$$k_1 \sin(\theta_1) = k_2 \sin(\theta_2) \quad (2.8)$$

This equation is known as *Snell's Law* and applicable to all waves. For pressure waves there are other more specific boundary conditions to take in to account. When the wave encounters an interface, the pressure and the normal displacement of that wave at the interface must be continuous [3]. The pressure boundary condition connects the amplitudes of the pressure waves such that $A_1 + A'_1 = A_2$ and the reflection and transmission coefficient are defined as

$$R = \frac{A'_1}{A_1} \quad \text{and} \quad T = \frac{A_2}{A_1} \quad (2.9)$$

The expression for the continuity of the normal displacement depends on the the angle between the displacement and the normal and is given as $\nu_1 \cos\theta_1 - \nu'_1 \cos\theta'_1 = \nu_2 \cos\theta_2$. Combining this expression with equation 2.9, taking into account that $\theta_1 = \theta'_1$ and that $\nu = \frac{p}{\rho c}$ [3], the solutions for the reflection and transmission coefficient become

$$R = \frac{\rho_2 c_2 \cos\theta_1 - \rho_1 c_1 \cos\theta_2}{\rho_2 c_2 \cos\theta_1 + \rho_1 c_1 \cos\theta_2} \quad \text{and} \quad T = \frac{2\rho_2 c_2 \cos\theta_1}{\rho_2 c_2 \cos\theta_1 + \rho_1 c_1 \cos\theta_2} \quad (2.10)$$

As mentioned before, in this research a piezo-electric tranducer produces a pulse that is guided through a rod. This pressure wave reflects on the interface between the rod and the liquid and is measured by the transducer. This is called the pulse-echo method. For the calculation of the density the acoustic impedance has to be calculated and is used to give another expression for the reflection coefficient. The acoustic impedance is defined as the ratio between the pressure and the velocity of the particles in the medium [3]. If this equation is combined with the former used expression of normal displacement, $\nu = \frac{p}{\rho c}$, the acoustic impedance can be expressed in density and sound velocity of the specific medium.

$$Z = \frac{\hat{p}}{\hat{v}} = \rho c \quad (2.11)$$

The reflection coefficient and the transmission coefficient can now be expressed in the acoustic impedances belonging to the specific mediums and this gives as a final result

$$R = \frac{Z_2 \cos \theta_1 - Z_1 \cos \theta_2}{Z_2 \cos \theta_1 + Z_1 \cos \theta_2} \quad \text{and} \quad T = \frac{2Z_2 \cos \theta_1}{Z_2 \cos \theta_1 + Z_1 \cos \theta_2} \quad (2.12)$$

2.3 Thermodynamic property calculations

In this section the calculations of the the thermodynamic properties density and viscosity are explained. The density of a certain fluid is derived using the reflection coefficient, equation 2.12. The acoustic impedance of the fluid, Z_1 , is separated from acoustic impedance of the solid, Z_2 , and the reflection coefficient, R_s , corresponding to the two media. Z_1 is expressed in its density, ρ_F , and its speed of sound, c_F . This gives the following expression for the density of the fluid

$$\rho_F = \frac{Z_2 (1 - R_s)}{c_F (1 + R_s)} \quad (2.13)$$

To calculate the density of the fluid R_s and c_F have to be found. Z_2 is already known because a copper rod is used and its properties are available already. To find c_F a pulse has to be propagated through the waveguide and the liquid. When the initial pulse reaches the solid-liquid interface a part of the wave is transmitted and a part is reflected. The reflected wave returns at the transducer at time t_1 . The transmitted wave first travels the distance from the end of the rod to the bottom of the crucible, reflects on the bottom, travels back and returns to the transducer at time t_2 . The wave that arrived at t_2 travelled a longer distance than the wave that arrived at t_1 . Thus to calculate the wave speed in the fluid c_F the difference in distance has to be divided by the difference in time

$$c_F = \frac{2l}{t_2 - t_1}, \quad (2.14)$$

where l is the distance from the end of the rod to the bottom of the crucible. The only parameter missing is the reflection coefficient, R_s , corresponding to the fluid. It can be calculated using a reference measurement with a reference material. When a ultrasonic wave, with an initial amplitude A_0 , travels through a solid it has a certain attenuation. This depends on the travelled distance of the wave in the waveguide. The pulse loses intensity when reflected at the interface of the sample fluid. The amplitude of the reflected wave can be described as

$$A_s = A_0 e^{-\alpha_{solid} 2l_{rod}} R_s \quad (2.15)$$

The equation for the reference material, water for instance, has a different reflection coefficient R_r and thus a different reflected amplitude A_r .

$$A_r = A_0 e^{-\alpha_{solid} 2l_{rod}} R_r \quad (2.16)$$

It is now possible to express R_s in the parameters A_s , A_r and R_r solely. If water is used as a reference material all the parameter are known because A_s and A_r can be measured and R_r can be calculated using equation 2.12.

$$R_s = \frac{A_s}{A_r} R_r \quad (2.17)$$

This is the equation for the calculation of the reflection coefficient and with this result ρ_F can be calculated.

For the calculation of the viscosity equation 2.6 will be used. The parameter ω , ρ and c are all known and only the attenuation coefficient α of the fluid has to be found. This coefficient can be found by measuring the ultrasonic pulse that went through the rod and the fluid and back. An approximation of the amplitude of this pulse is given as

$$A_{s1} = A_0 e^{-\alpha_{solid} 2l_{rod}} (1 - R_s)^2 e^{-\alpha_{fluid} 2l_1} \quad (2.18)$$

In this equation A_0 is the initial amplitude, l_{rod} is the length of the rod, l_1 the distance from the end of the rod to the bottom of the crucible and $(1 - R_s)^2$ is the transmission coefficient squared because the pulse crosses the interface twice. To calculate the attenuation coefficient α_{fluid} a second pulse measurement should be done but with a different immersion depth, so l_1 is changed. This gives

$$A_{s2} = A_0 e^{-\alpha_{solid} 2l_{rod}} (1 - R_s)^2 e^{-\alpha_{fluid} 2l_2}, \quad (2.19)$$

where l_2 is a different immersion depth than l_1 . In the equations 2.18 and 2.19 the first three terms are the same for the two different measurements and can therefore be expressed in one another. By doing this the attenuation coefficient of the solid does not have to be calculated.

$$\frac{A_{s1}}{e^{-\alpha_{fluid} 2l_1}} = \frac{A_{s2}}{e^{-\alpha_{fluid} 2l_2}} \quad (2.20)$$

This equation can be rewritten in to final expression for the calculation of the attenuation coefficient for the fluid

$$\alpha_{fluid} = \frac{1}{2(l_2 - l_1)} \ln \left(\frac{A_{s1}}{A_{s2}} \right) \quad (2.21)$$

This attenuation coefficient is used for calculation of the viscosity using equation 2.6.

2.4 Surface acoustic waves

Waves which travel along the interface between two media are called surface waves. There are several different surface waves and their characteristics depend on the media in which they propagate. The Rayleigh wave travels on vacuum-solid surfaces [12]. This wave has both a longitudinal and transverse motion and a phase difference exists between these two motions. Therefore the particles on and near the surface make an elliptical movement. The particle displacement decays exponentially with depth. Rayleigh waves are non-dispersive and this makes that their phase velocity is independent of the frequency [13]. The Stoneley wave is a wave which travels on the solid-solid interface. These waves decay exponentially into both solids. The Scholte wave travels on the solid-liquid interface [12]. In this domain also leaky Rayleigh waves are present which dissipate energy into the liquid.

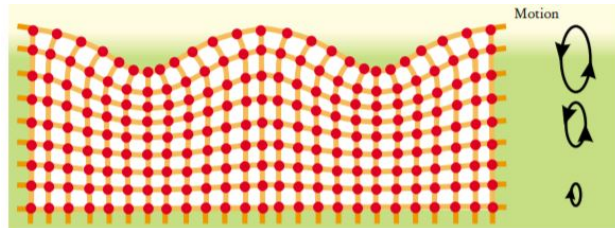


Figure 2.1: Rayleigh wave [13].

Cegla et al. [14] discussed a method for measuring material properties using Rayleigh and quasi-Scholte waves. The quasi-Scholte wave asymptotes the Scholte-interface wave behaviour at high frequencies. The attenuation of the quasi-Scholte wave is caused by shear leakage and bulk longitudinal attenuation of the embedding material. This attenuation is important for the calculation of the viscosity of the fluid. A shear transducer produces and excites an A0 (anti-symmetrical) wave along a thin plate dipped in a fluid, see figure 2.2. When the surface wave hits the solid-liquid interface a part of the wave is reflected and remains a Rayleigh wave. The transmitted wave is converted to a Scholte wave and leaky Rayleigh waves. This wave eventually reflects at the end of the rod and will return to the transducer. This is an alternative way of measuring thermodynamic properties using surface acoustic waves. The calculation method for the reflection coefficient and attenuation coefficient however, described in equation 2.17 and 2.21 respectively, remains the same. An advantage of this method is that only the length of the rod has to be taken into account. A more comprehensive explanation can be found in Cegla et al. [14] (Thesis of Cegla).

The same can happen with the propagation of a shear wave in the waveguide. A shear horizontal mode is propagated in the same direction along the waveguide but has a polarisation direction perpendicular to the propagation direction. Also this mode is highly attenuated when the waveguide is immersed in the fluid.

2.5 Dispersion

An ultrasonic pulse, wave packet, consists of a superposition of several waves with different amplitudes and frequencies. When a pulse travels through a waveguide these different frequency components can have different wave velocities called phase velocity c_{ph} . The wave packet as a whole has a velocity as well and is called group velocity c_g . These velocities can be described as [15]

$$c_{ph} = \frac{\omega}{k} \quad \text{and} \quad c_g = \frac{\partial \omega}{\partial k}, \quad (2.22)$$

where ω is the angular frequency and k the wave number. If the phase velocities of the different frequency components have the same velocity as the group velocity, no dispersion occurs and the shape of the pulse will be conserved. In this situation the phase velocity is constant.

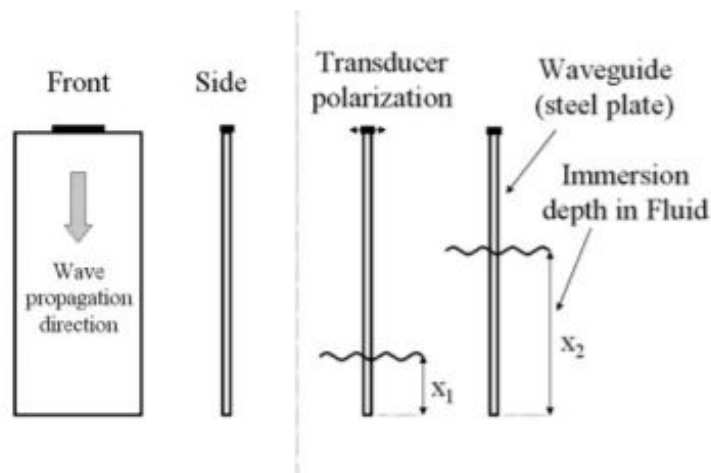


Figure 2.2: Schematic of the 'dipstick' method [14].

But if such a pulse propagates along a distance through a waveguide which is a dispersive medium, the frequency components will travel at different velocities. This creates a more stretched pulse shape with lower amplitudes. The phase velocity is not constant but a function of frequency $c_{ph} = c_{ph}(\omega)$. This type of dispersion makes it more difficult to calculate the correct value of the pulse at a later stage of time and reduces the propagation range and the signal to noise ratio [16]. Dispersion in a system can be increased by scattering and absorption in a medium that is not fully isotropic. The residual-resistance ratio (RRR) can be used as a purity scale. The RRR is a ratio defined as the ratio between the density of the material at room temperature and at (almost) zero Kelvin [17]. The more dense the material at room temperature, the more pure the material is. This implies a higher residual-resistance ratio, which should mean less impurities and thus less dispersion caused by scattering.

$$RRR = \frac{\rho_{300K}}{\rho_{0K}} \quad (2.23)$$

There are several ways of reducing the dispersion a measuring set up. If a wave packet is sent through a waveguide of a certain length, the dispersion can be reduced by shorten the length of the waveguide. The smaller the propagation distance, the less time the pulse has to disperse. Also, the frequency-thickness has a role in the creation of dispersion. Less higher mode waves are created at low frequency-thickness. Another way of reducing dispersion is the technique of time-reversal in an ultrasonic waveguide [17]. The time-reversal technique means that for every dispersed pulse which is received at a receiver, there exist in theory a set of waves that retraces all paths and converges in the original source. With this technique the waves and their deformation in time are evaluated in order to trace back which part of the original pulse corresponds to which part of the dispersed wave. Thus dispersed pulses can be converted to their undispersed shapes and better measurements can be done. A more extensive explanation can be found in Roux et al. [17].

Chapter 3

Experimental and simulation method

This research focuses on the measurement method of thermodynamic properties such as density and viscosity of the molten salt fluid. There are multiple ways to measure density or viscosity. For instance, the falling body technique makes it possible to determine the viscosity by the time a body takes to fall through the fluid. With the rotational technique the torque necessary for turning an impeller in a viscous fluid is proportional to this viscosity. A method based on the propagation of ultrasonic waves can also be used. With the last mentioned one the reflection coefficients and the fluids attenuation coefficient have to be calculated. To develop a measuring method it is important to know what are the criteria and boundary conditions of the system. The most important criteria in our case is that the molten salt is radioactive and very hot. This means that only a small amount of the fluid can be used, also because of its high density, and that materials used for the measurement have to withstand this radioactivity and heat. The falling body and rotational measuring techniques are therefore not ideal because of the small amount of fluid available. Also, the density has to be calculated and these two measurement methods only measure the viscosity. To measure the density an independent measurement has to be done and this is undesirable. With ultrasonic waves, the density and viscosity of the molten salt can be measured with the same measurement. A small sample is enough for an accurate measurement and by using a waveguide the heat from the fluid can be dissipated. Therefore ultrasonic waves with a waveguide are used in this research for the measurement of density and viscosity.

In this chapter the experimental set up, simulation method and the experimental method are discussed and explained. The first section gives a description of the real experiment to give a good outline of how the simulation should be modeled. After this section the creation of the simulation will be covered. The simulation will be done with the program COMSOL 5.2a Multiphysics [10].

3.1 The experimental set up

In this research the focus lies on the measurement of the density and viscosity of the molten salt of a MSFR. A new type of viscometer has to be created using ultrasonic waves with a waveguide. In these experiments no radioactive molten salt will be used, because this is not available and the system should be optimised first to correct for errors that might interfere with the measurements. The measurement method can be described as a pulse-echo measurement which also enables the measurement of the speed of sound in the liquid. This value is necessary for the calculation of the viscosity.

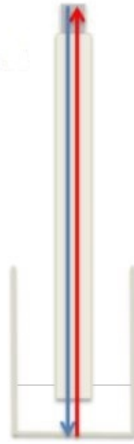


Figure 3.1: Schematic set up of the rod, transducer and liquid [3].

The general idea of this research is to send an ultrasonic pulse through a wave guide which is in contact with the liquid in the container, see figure 3.1. The pulse is created using a piezoelectric transducer on top of the waveguide. When the pulse is reflected, it will be detected by the transducer acting as both pulser and receiver. The left wave is the incoming wave and the right wave is the reflected wave from the bottom of the crucible. For the calculation of the density and the viscosity of the liquid the reference measurement, the measurement of the reflected wave from the liquid-solid interface and the measurement of the transmitted wave are important.

The reflection coefficient between a solid and a liquid depends on the corresponding acoustic impedances. Their relation is expressed in equation 2.12. A high transmission coefficient and thus a low reflection coefficient is desirable because in that way more signal will reach the fluid and does not fade away in the noise. The waveguide in this case is made of copper. The reason that copper is used is that it is a common metal and available. In this first stage, tests are done with this material already. Preferably, in later studies ceramics such as boron nitride or metals like nickel will be used. These materials will withstand the corrosivity, the high temperature and have acoustic properties compatible with the fluid. The properties of copper and boron nitride are shown in table 3.1. The acoustic impedances of fluid are important as well, because a higher acoustic impedance causes lower reflection coefficient. Therefore glycerol is chosen as measuring fluid because it has a higher acoustic impedance than water and is available. As discussed in the Theory section a reference measurement is necessary for the calculation of the reflection coefficient of the liquid-solid interface. The reference fluid in this case is water with a reflection coefficient of 0.93 with copper [3]. The normal measurement is done with glycerol which has a reflection coefficient with copper of 0.89 [3]. Other properties of water and glycerol are displayed in table 3.1.

Table 3.1: Physical and acoustic properties of copper, boron nitride, water and glycerol with ρ density, μ viscosity, c sound velocity and Z acoustic impedance [3].

Material	ρ [k/m ³]	μ [mPa s]	c [m/s]	Z [M Rayl]
Copper	8960	-	4600	41.2
Boron Nitride	2100	-	16653	35
Water	1000	0.89	1480	1.5
Glycerol	1260	950	1920	2.4

3.2 The simulation method

The simulation part of this research is done using COMSOL 5.2a Multiphysics [10]. The physics modeling in COMSOL follows a standard work flow. The sequence of steps to take in order to make a simulation is always the same. First, set up the model environment, create geometric objects, specify material properties, define physics boundary conditions, create the mesh, run the simulation and post-process the results. This sequence will also be used as a set up for this section.

3.2.1 The model environment

To simulate an ultrasonic pulse through a copper waveguide in contact with a liquid, the Acoustic-Solid interaction interface is used. It combines the Pressure Acoustics and Solid Mechanics interfaces to connect the pressure variations in the fluid domain to the structural deformation in the solid domain. The Acoustic-Solid interaction interface of COMSOL automatically defines fluid-solid boundary conditions. This is done in 2D but it can be extended to 3D, which works with the same steps.

3.2.2 Create geometric objects

A solid domain and a liquid domain have to be created with the correct dimensions to simulate the rod and liquid. Under the tab Geometry these domains can be specified. A rectangular domain is used to build the solid and fluid domain. Its dimensions are defined in Parameters using Global Definitions in Model Builder. All the parameters that are being used in this simulation are defined in that tab and the values can be found in Appendix A, some are changed during the project. The solid domain is on top of the liquid domain so that their adjacent boundaries overlap, see figure 3.2. This combined boundary couples the fluid and solid interface and the different physics of these interfaces.

3.2.3 Specify material properties

Materials can easily be selected using the build-in material library in COMSOL. For the created rod, copper with the residual-resistance ratio of 30 is used. The residual resistance ratio is an index of the purity of the material. For these simulations water and glycerol are used as fluids. The properties that were used in COMSOL are stated in table 3.1.

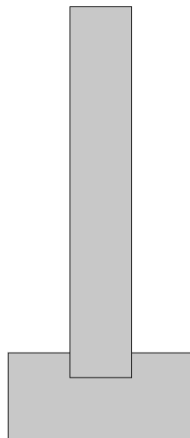


Figure 3.2: Rod immersed in liquid created in COMSOL.

3.2.4 Define physics boundary conditions

The whole simulation depends on valid choices for the boundaries conditions of this geometric object. In order to create a pulse on top of the rod, on this boundary a Prescribed Displacement in the y-direction is placed. The pulse is a Gaussian because a finite pulse has to be created. The frequency of this pulse is 2 MHz. In the real experiment a pulse frequency of 3.5 MHz is used. If this frequency was used in the simulation, the computation time would almost double. This pulse is shown in figure 3.3. The boundaries of the rod that are not in contact with the liquid domain are given Free Boundaries. This means that there are no constraints and no loads acting on the boundary. The boundary between the solid domain and liquid domain is coupled automatically by COMSOL as already stated in section 3.2.1.

3.2.5 Create the mesh

For the creation of the mesh certain conditions were taken into account. The mesh has to be fine enough to give a reasonable representation of the rod-fluid system, but not too fine because of the limited computing power and computing duration. The mesh elements are outlined on the boundaries of the liquid and solid domain, which form a quadrilateral mesh shape. For the first simulations in the 2D model five elements per wave length were used [18]. This is the minimum number mesh elements for measuring correct results because the Nyquist limit states that a sampled waveform needs at least two sample points per cycle [19] in order to avoid aliasing. The amount of mesh elements can be calculated by dividing the length of the waveguide by the wavelength of the longitudinal pressure wave times of mesh elements one wants per wavelength. The optimal number of mesh elements is eight [7] but this increases the computation time drastically. The liquid domain is at first defined as a Free Triangular mesh, a build-in domain mesh maker.

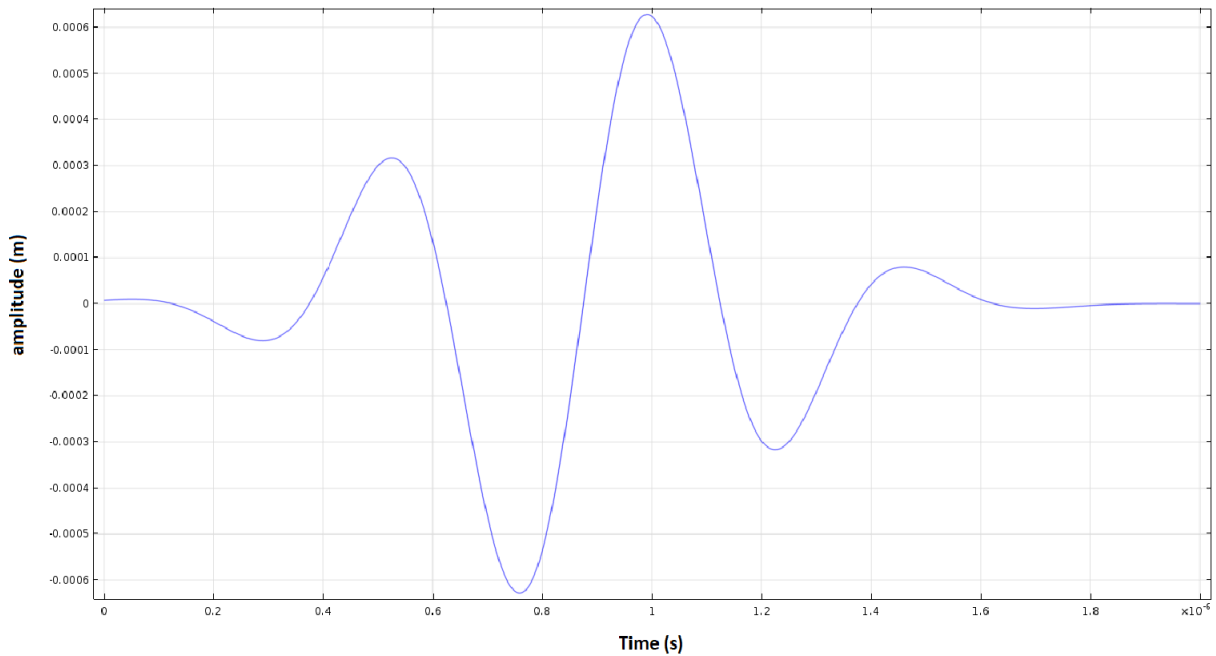


Figure 3.3: Gaussian Pulse created in COMSOL

3.2.6 Run the simulation and post-process the results

Before the simulation can be run a certain study has to be chosen to order to evaluate the simulation. In this case the Time Dependent study was chosen. The results from this study are collected in the tab Results and can be expressed in tables, plots, animations and graphs. The Time Dependent Study of COMSOL is a finite element method. In the program a start and end time should be given. It divides this time duration into smaller intervals and studies these intervals. These time intervals are defined in advance and are determined by the Courant–Friedrichs–Lewy (CFL) number: $CFL = c_l * \frac{\Delta t}{meshsize}$ [18]. This number gives the relationship between the mesh size and time step. The optimal value of the CFL number is 0.2 [18].

3.3 Experimental method

The results obtained with COMSOL have to be processed. This is done with the program MATLAB [20]. For the reflection coefficient calculation, and thus the density, the most important result is the first reflected peak from the solid-liquid interface. For every immersion depth two measurements have to be done: a reference measurement with the reference material, water in this case, and a normal measurement with the material of which the properties are investigated, glycerol. It is very difficult to link a certain reflected peak to the initial pulse. Therefore the intensity over a broader area of the pulse is taken to give a better estimation. These intensities are used to calculate the reflection coefficient using equation 2.17. Depending on the outcome of the results, attempts are done to optimise and improve the simulation to eventually give a better representation of the real set up. The measurement of the attenuated pulse in the fluid, with a copper waveguide, is going to be very difficult because of the low intensity that probably returns to the transducer.

Chapter 4

Results and discussion

In this chapter the results are shown and discussed. The first simulation in 2D is done to find out how COMSOL and the solid-fluid system behave on the given input. Measurements in order to find the reflection coefficient are done. The data obtained from the COMSOL simulations are processed in Matlab [20].

4.1 2D model with immersion

In this section the results of the 2D simulation model are evaluated and discussed. In this simulation the copper rod has the length of 150 mm and a width of 25 mm. In the simulation five mesh elements per wavelength are used. These dimensions are the same as the dimensions of the rod used in the real experiment. The rod is immersed in the fluid from 0 mm to 20 mm with steps of 5 mm. For every immersion depth a reference measurement is done with water and a normal measurement is done with glycerol. Two measuring probes are used: one at the top of the rod, at the position of the transducer, and one at the solid-liquid interface. The most important calculation of the reflection coefficient of the fluid is done with the probe at the top of the rod. The probe at the solid-liquid interface is used to check the reflection coefficient of the liquid via the transmission coefficient. The result of this second probe is more reliable than the first probe because one can measure directly after the wave propagated through the boundary. However, the reflection coefficient has to be measured at the top of the rod, thus the results of the second probe are mainly used as a reference. The theoretical value of the reflection coefficient of glycerol is 0.89 and the theoretical reflection coefficient of water is 0.93. These values are used to calculate the deviation of the results from the theoretical value. The calculated reflection coefficients from the probe at the top and the probe at the solid-liquid interface and their deviations are shown in table 4.1.

Table 4.1: The reflection coefficients of a straight copper rod with length 150 mm and width 25 mm immersed in glycerol and deviations from theoretical reflection coefficient value 0.89. Five mesh elements per wavelength are used.

Immersion depth [mm]	0	5	10	15	20
Reflection coefficient top probe	0.974	0.751	0.797	0.968	0.715
Deviation from theoretical value	9.422%	15.667%	10.482%	8.795%	19.774%
Reflection coefficient bottom probe	0.930	0.918	0.942	0.935	0.926
Deviation from theoretical value	4.526%	3.113%	5.818%	5.032%	4.046%

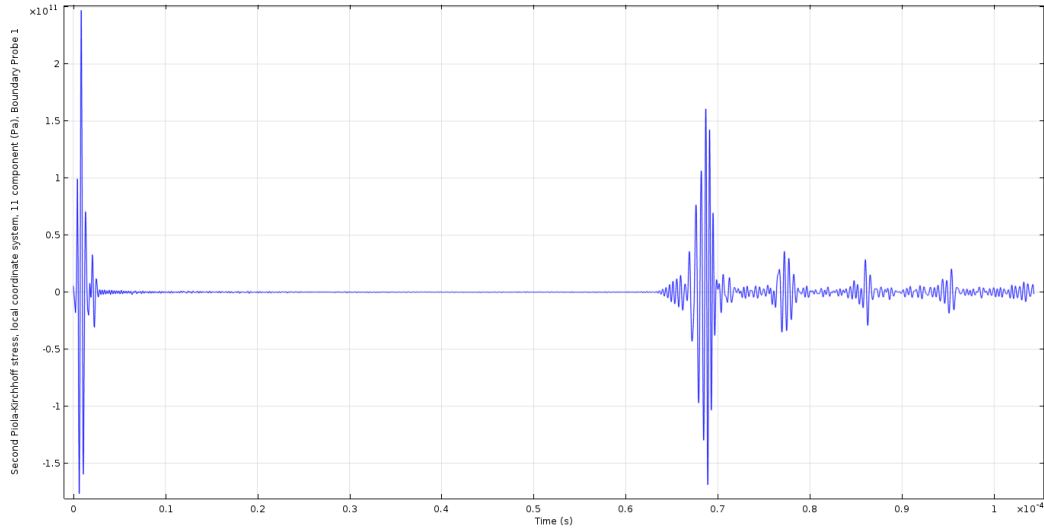


Figure 4.1: Plot of a pulse measurement at the top probe of a straight copper rod with length 150 mm and width 25 mm immersed 5 mm in glycerol. Five mesh elements per wavelength are used.

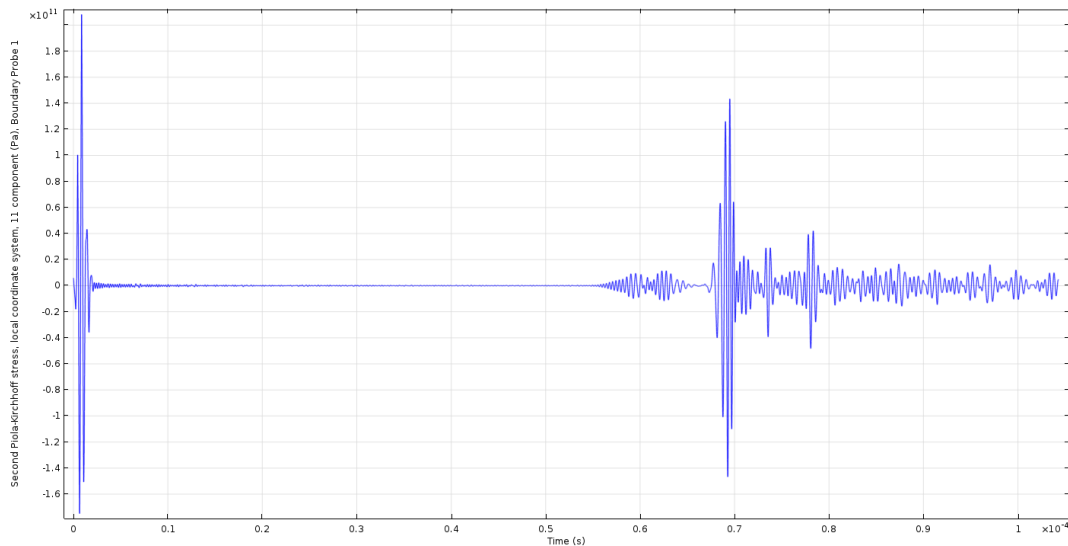


Figure 4.2: Plot of a pulse measurement at the top probe of a straight copper rod with length 150 mm and width 25 mm immersed 20 mm in glycerol. Five mesh elements per wavelength are used.

The reflection coefficients calculated at the top probe deviate about 9-20% from the theoretical value and this is obviously too much when looked at the deviation of the bottom probe (3-6%). In addition to these results two top probe measurements, one at 5 mm and one at 20 mm immersion depth, are shown in figure 4.1 and figure 4.2. In these two figures the initial pulse can be seen near the zero of the time axis. The second large pulse of both the figures is the reflected pulse from the solid-liquid interface. In both figures trailing echoes were measured. These echoes travel behind the initial pulse but have smaller intensity, this can be seen clearly in figure 4.1 but they also exist in the pulse measurement in figure 4.2. When the initial pulse at the top of the rod is created, surface waves, which propagate on the boundary of the rod, are made. These waves reflect on the

solid-liquid interface as well. When the rod is immersed deeper in the liquid, the unimmersed part of rod becomes shorter and thus the reflected surface wave returns faster at the transducer. In figure 4.2 this reflected surface wave can be spotted very clearly in front of the second large peak. In figure 4.1 this reflected surface wave is less obvious. The surface waves and trailing echoes cause unwanted loss of intensity. This makes the calculated reflection coefficients of table 4.1 deviate from the theoretical value of 0.89 for glycerol. The values of the reflection coefficient at the zero and fifteen immersion depth even are above the theoretical value. This however is caused by way the measured results where processed. In this process the peaks of a reflected pulse are summed over a time domain. This time domain can vary depending on the amount of dispersion the reflected pulse has. If a signal has a lot of dispersion, the measuring process can give the result that the intensity of the reflected pulse at the glycerol interface is higher than the intensity of the reflected pulse at the water interface, which is not correct.

In the next section a new 2D model is simulated without the rod immersion in order to eliminate the surface waves and improve the simulation.

4.2 2D model without immersion

In order to improve the previous simulation, a new 2D model is made without the rod being immersed in the liquid to avoid surface waves, which take away intensity. For the calculation of the reflection coefficient of a liquid it makes no difference whether or not the rod is dipped in the fluid or that the solid and liquid boundaries only touch with decreasing liquid depth. The same measuring method and measurements as in the previous section are executed and the results are shown in table 4.2.

The results of table 4.2 deviate more from the theoretical value than the results of table 4.1. The measuring method is not improved. The new model did not have the desired effect on the reflection coefficients of the top probe. The values of the coefficients are not near the theoretical value of glycerol. A reason why these coefficients still deviate from the correct value could be that measurements were done with five mesh elements per wavelength instead of the optimal eight mesh elements per wavelength. Five mesh elements was initially chosen because it should give a representation of the pulse in the system and has the lowest computation time. It is possible that only using five mesh elements per wavelength can give a false representation of the pulse in the measurement. To further clarify, in figure 4.3 and figure 4.4 pulse measurements of the top probe are shown of water and glycerol at a decreased fluid depth of 5 mm. The reflected pulse of water in figure 4.3 is substantially larger than the reflected pulse of glycerol in figure 4.4.

Table 4.2: The reflection coefficients of a straight copper rod with length 150 mm and width 25 mm without immersion in glycerol and deviations from theoretical reflection coefficient value 0.89. Five mesh elements per wavelength are used.

Decreased fluid depth [mm]	0	5	10	15	20
Reflection coefficient top probe	0.664	0.662	0.711	0.720	0.739
Deviation from theoretical value	25.342%	25.673%	20.098%	19.049%	16.964%
Reflection coefficient bottom probe	0.917	0.927	0.907	0.889	0.870
Deviation from theoretical value	3.037%	4.182%	1.913%	0.091%	2.263%

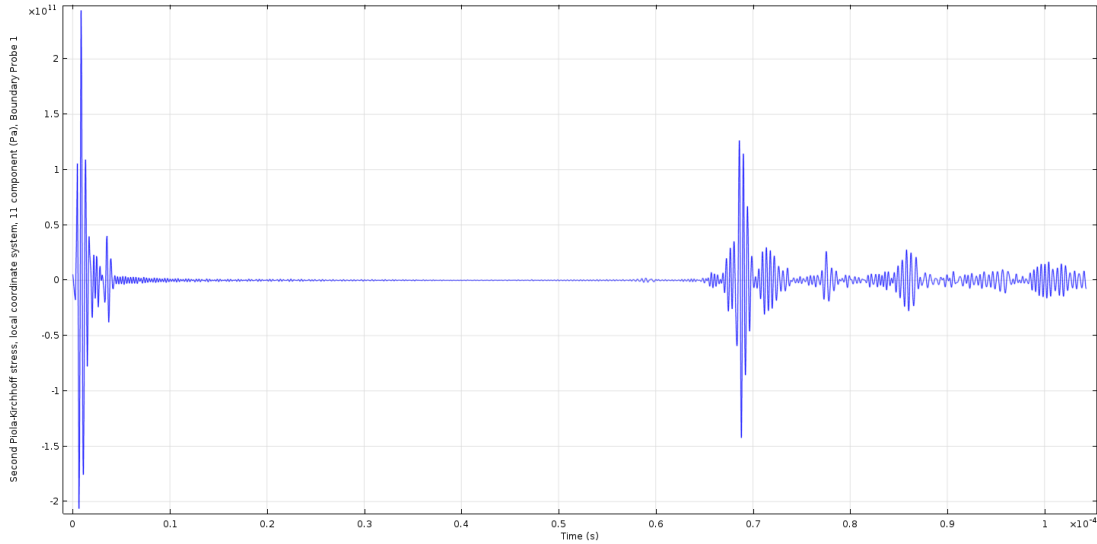


Figure 4.3: Plot of a pulse measurement at top probe of a straight copper rod with length 150 mm and width 25 mm at 5 mm decreased liquid depth in water. Five mesh elements per wavelength are used.

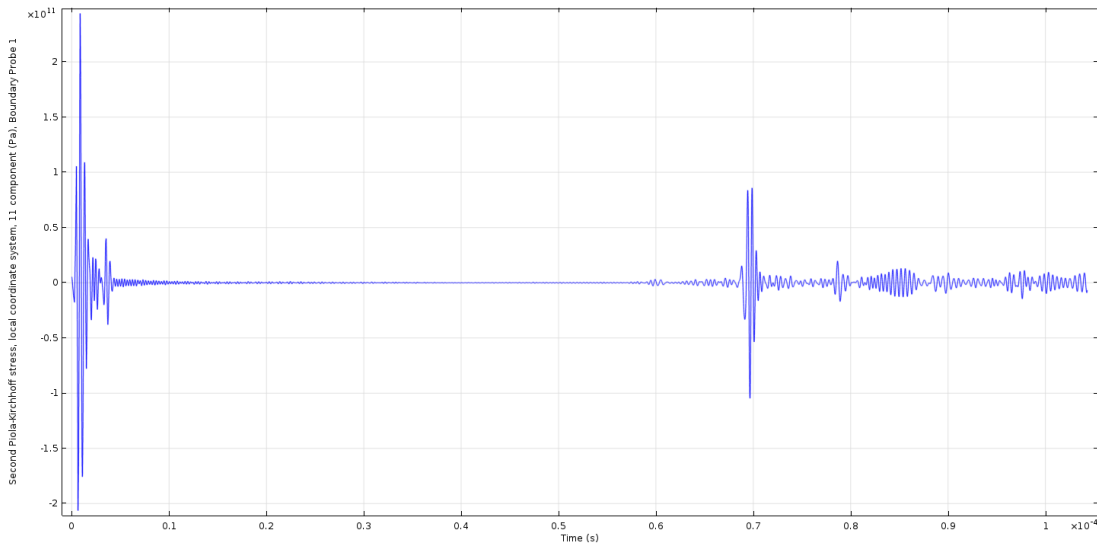


Figure 4.4: Plot of a pulse measurement at top probe of a straight copper rod with length 150 mm and width 25 mm at 5 mm decreased liquid depth in glycerol. Five mesh elements per wavelength are used.

Based on the results of the tables 4.1 and 4.2 it cannot be concluded that the immersed simulation set up is worse than the unimmersed set up. It is highly probable that large deviation between the two is caused by the wrong number of mesh elements per wavelength. But the assumption that the unimmersed set up should give a higher intensity due to the lack of created surface waves is unchanged. This high intensity is important for the calculation of density and viscosity and therefore the unimmersed set up will be used in the following set ups. In order to improve the results, in the next section several measures are taken that eventually should improve these results.

4.3 Measurement method optimisation

To check if the correct number of mesh elements per wave length is used, a mesh convergence calculation is done. A point near the solid-liquid interface is chosen as measurement point. The quantity that will be measured is the pressure. First the simulation is done for one mesh element per wavelength, then two mesh elements per wavelength till eight mesh elements per wavelength. The difference between the results per mesh elements and the highest number of mesh elements is done to create a convergence to approximately zero. The mesh convergence plot is shown in figure 4.5. This figure shows that from six mesh elements per wavelength the difference becomes stable near zero. This means that the measurements with five mesh element per wavelength are not correct and this explains why the results from table 4.2 deviated significant from the theoretical value. This result is also found by previous research [7] and current research.

To improve the measurement method, the number of mesh elements per wavelength is increased from five to eight. The expectation is that the results will give a more accurate representation of the wave propagating in the waveguide. The simulations are done with the same rod dimensions of the former simulations and with no immersion in the liquid. The fluid for this simulation is water. In figure 4.6 this simulation is shown.

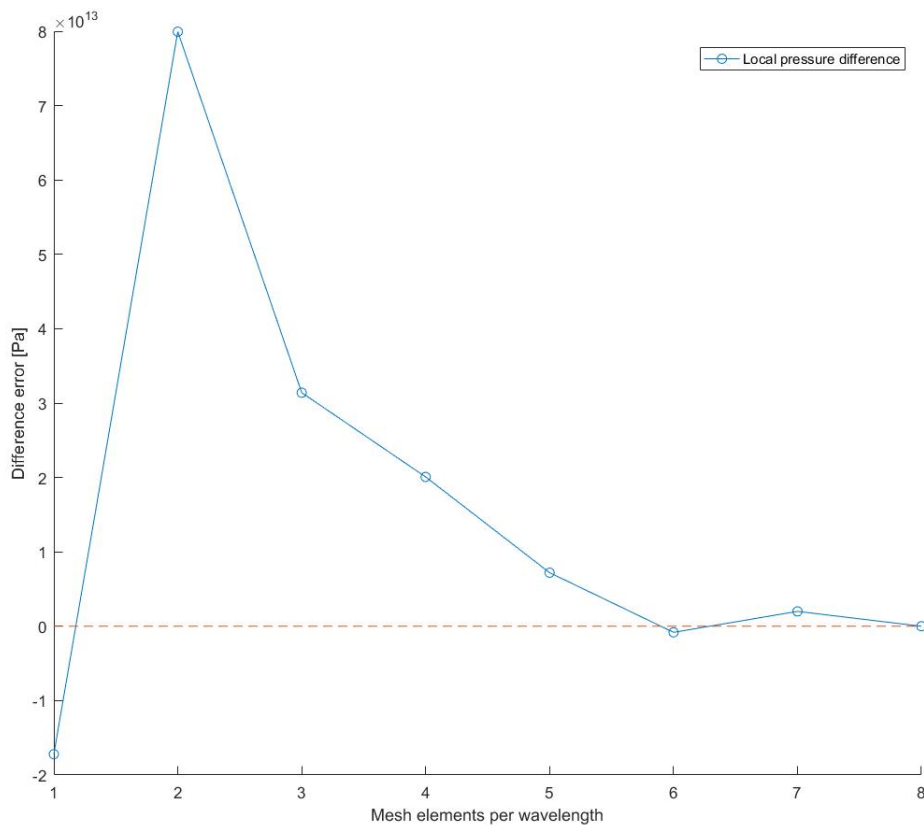


Figure 4.5: Mesh convergence plot with data from a selected point from near the solid-liquid interface.

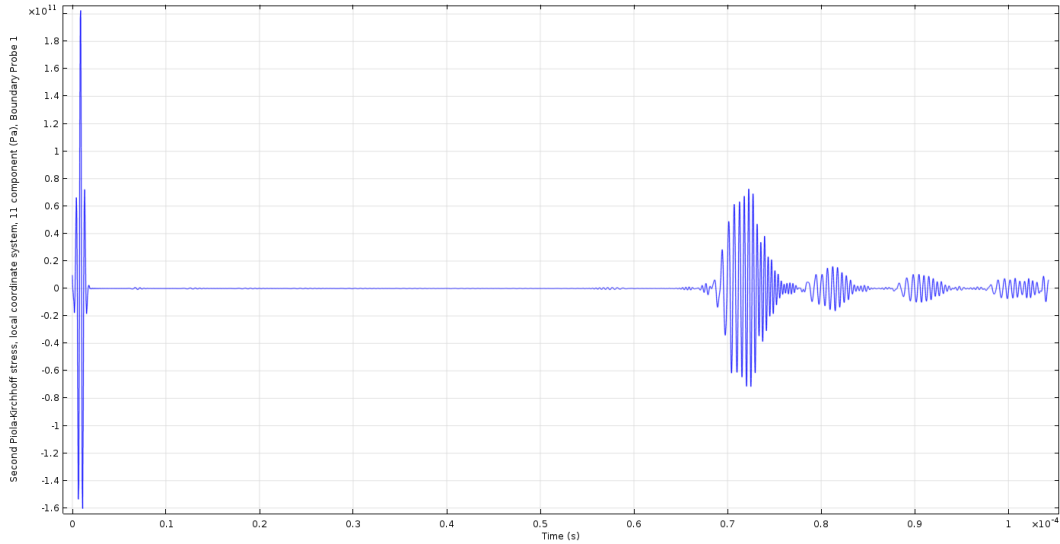


Figure 4.6: Plot of a pulse measurement at top probe of a straight copper rod with length 150 mm and width 25 mm without immersion in water. Eight mesh elements per wavelength are used.

The result from the measurement shown in the figure 4.6 is too dispersed to do an accurate calculation of the reflection coefficient. This large dispersion can be caused by the length of the copper rod. Therefore the copper rod is shortened to counter the large dispersion of this simulation. The length of the rod is shortened from 150 mm to 100 mm and the width from 25 mm to 17 mm. The result of this simulation is done with water as liquid and shown in figure 4.7. In this figure it can be seen that the reflected pulse is still dispersed, but less and its intensity can now be calculated. This dispersion can be caused by scattering or absorption in a medium that is not fully isotropic. Therefore the residual-resistance ratio of the copper is increased from 30 to 3000. Everything else from the simulation set up remains the same. The result is displayed in figure 4.8.

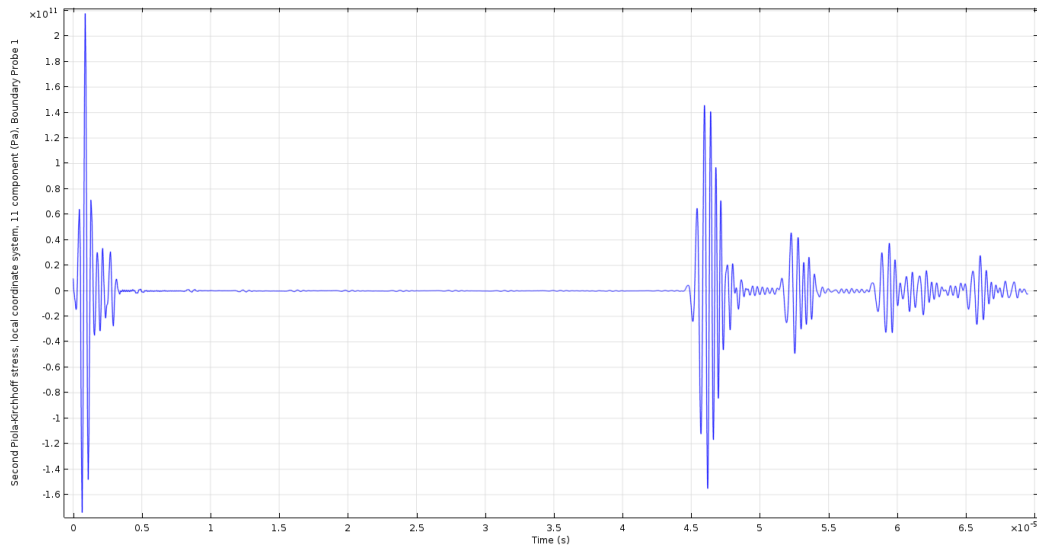


Figure 4.7: Plot of a pulse measurement at top probe of a straight copper, $RRR = 30$, with length 100 mm and width 17 mm without immersion in water. Eight mesh elements per wavelength used.

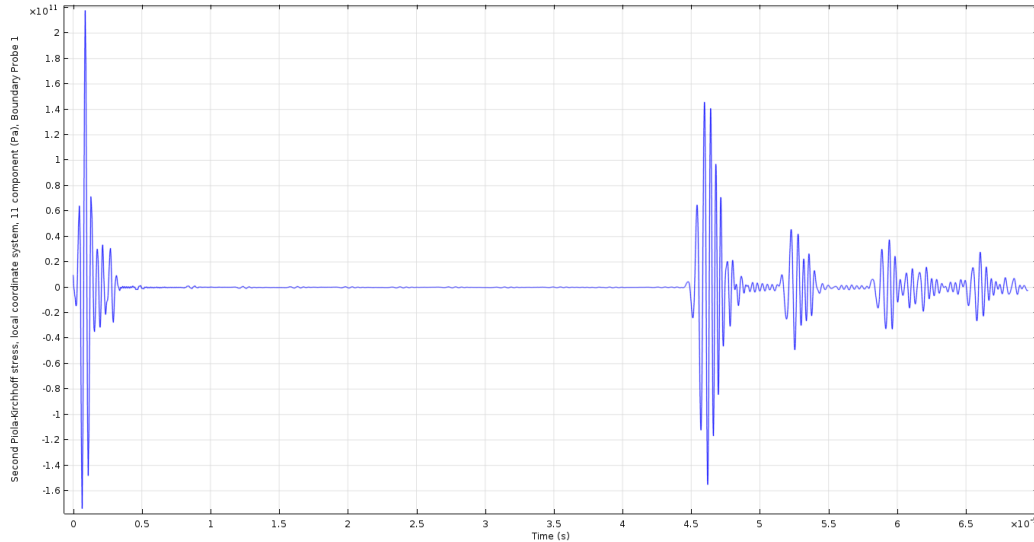


Figure 4.8: Plot of a pulse measurement at top probe of a straight copper, $RRR = 3000$, rod with length 100 mm and width 17 mm without immersion in water. Eight mesh elements per wavelength are used.

In figure 4.7 and 4.8 no difference can be seen between the plots. From this result can be deduced that the dispersion in this simulation is not caused by scattering or absorption but purely by the length of the rod. The dispersion in this pulse measurement is not insuperable, the intensity of this pulse can be calculated summing over a broader time interval. The changes in the measurement set up will probably improve the measurement of the reflection coefficient. In the next section, measurements are done to confirm this.

4.4 2D model without immersion; smaller waveguide

In this model the length of the copper rod is shortened from 150 mm to 100 mm to make sure it has a noticeable effect on the dispersion. Its width is shortened from 25 mm to 17 mm. The initial depth of the fluid is 15 mm and will decrease to 5 mm with steps of 2.5 mm. Water, as reference material, and glycerol are used in these measurements. Ten measurements are done, two at every depth for the two different fluids. Only top probe measurements are done. The results of these measurements are shown in table 4.3.

The results of the reflection coefficients of the top probe have improved. The shortening of the rod and increasing of the mesh per wavelength have caused that the results begin to approach the theoretical value of 0.89. The deviation of the calculated reflection coefficient from this value is between 1.5-12.3% and thus improved in contrast to the results of section 4.1 and section 4.2. In figure 4.9 and 4.10 the measurements of water and glycerol are shown at a decreasing depth of five millimeter.

With these values of the reflection coefficient between glycerol and copper and the speed of sound, the density of glycerol can be calculated using equation 2.13. The deviation of the calculated glycerol density will be proportionally the same as the deviation of the measured reflection coefficient of glycerol. The following step in the process is to calculate the attenuation coefficient of

acoustic wave in glycerol. In order to accomplish this the speed of sound in glycerol must be calculated using equation 2.14. This value was already stated in table 3.1 and can be used as theoretical value, namely: $c = 1920$ m/s. For the calculation of the attenuation coefficient, measurements of the intensities of the waves which have propagated through the liquid have to be done. Note that this is a different received pulse than the reflection coefficient pulse. The pulse that should be measured travels through the waveguide into the liquid, reflects there and travels back to the waveguide to the receiver. These intensities can be small because they have crossed the solid-liquid interface twice and therefore have lost a lot of intensity. The problem that can arise with this system is the fact that the trailing echoes can cause a lot of noise in the calculation of this properties, contrary to the calculation of the reflection coefficient. The solution to this problem is to simulate a tapered rod instead of a straight one. In previous research [9] this has been done and an optimal tapering angle of 1.25° had been found. After the trailing echoes are minimised the prospect is that the intensities of the waves which propagated through the liquid can be found and processed. For the calculation of the attenuation coefficient according to equation 2.21, measurements of glycerol at different immersion depths have to be compared.

In the next section, measurements with the new simulation set up are described. The rod is tapered with an angle of 1.25° in these simulations. The acoustic wave speed in the liquid was determined and measurements at different decreased fluid depths were executed.

Table 4.3: The reflection coefficients of a straight copper rod with length 100 mm and width 17 mm without immersion in glycerol and deviations from theoretical reflection coefficient value 0.89. Eight mesh elements per wavelength are used.

Decreased fluid depth [mm]	0	2.5	5	7.5	10
Reflection coefficient top probe	0.78	0.78	0.85	0.90	0.91
Deviation from theoretical value	12.36%	12.36%	4.49%	1.46%	2.25%

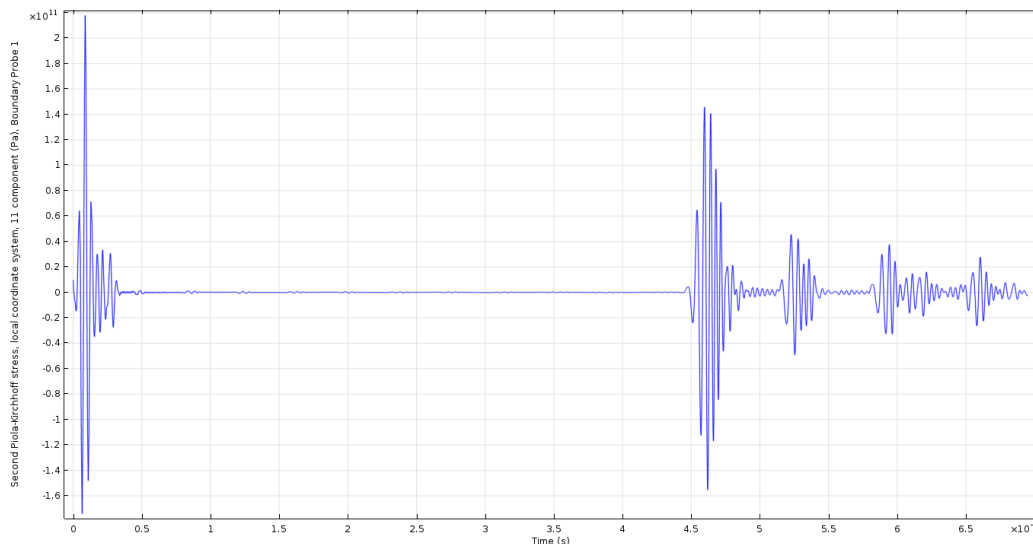


Figure 4.9: Plot of a pulse measurement at top probe of a straight copper rod with length 100 mm and width 17 at 5 mm decreased liquid depth of water. Eight mesh elements per wavelength used.

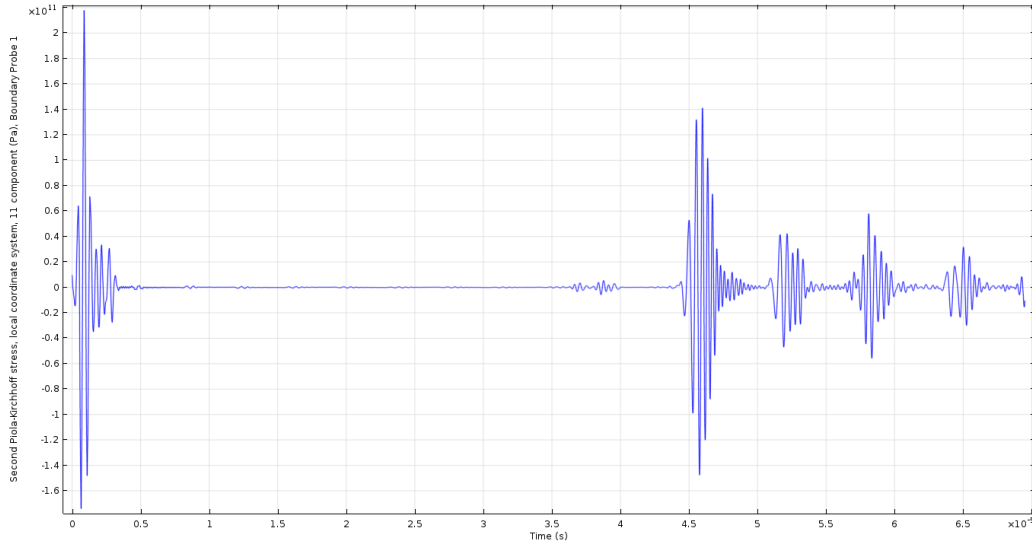


Figure 4.10: Plot of a pulse measurement top probe of a straight copper rod with length 100 mm, width 17 mm at 5 mm decreased fluid depth of glycerol. Eight mesh elements per wavelength used.

4.5 2D model without immersion; smaller tapered waveguide

In the new simulation model the length of the copper waveguide is 100 mm, its width 17 mm and has a tapering angle of 1.25° . The initial fluid depth is 17 mm. In order to do a calculation of the density and viscosity, the reflection coefficient, speed of sound in glycerol and the attenuation coefficient are measured. Again for the reflection coefficient, reference measurements with water are done. The calculation of the speed of sound in glycerol is done with the results of measurements with glycerol and using equation 2.14. For the calculation of the density, the calculated speed of sound in glycerol and the reflection coefficient are used in equation 2.13. The measured intensities of the transmitted waves are used to calculate the attenuation coefficient using equation 2.21. The calculation of the viscosity of glycerol can now be done using equation 2.6.

4.5.1 Density calculation

The results of the reflection coefficient shown in table 4.4 are near 0.89. The average of these results is taken in order to reduce the influence of fluctuations in the calculation of the coefficient. This average value comes close to the theoretical value and has a deviation of less than 1%.

Table 4.4: The reflection coefficients of a copper and the speed of sound in glycerol and their deviations are measured. The copper rod, with length 100 mm, width 17 mm and a tapering angle 1.25° , is not immersed in the glycerol. The theoretical reflection coefficient is 0.89 and the theoretical speed of sound in glycerol is 1920 m/s. Eight mesh elements per wavelength are used.

Decreased fluid depth [mm]	0	2.5	5	7.5	10	Average
Reflection coefficient top probe	0.88	0.85	0.92	0.93	0.83	0.882
Deviation from theoretical value	1.12%	4.49%	3.37%	4.61%	6.85%	0.90%
Speed of sound glycerol [m/s]	1985.6	1968.5	1917.7	1867.4	1947.1	1939.1
Deviation from theoretical value	3.42%	2.53%	0.12%	2.27%	1.41%	0.99%

Table 4.5: Calculated density values of glycerol for different chosen reflection coefficients and speed of sound in glycerol. The theoretical value of the density of glycerol is 1260 [kg/m³]

Depth of fluid [mm]	0	2.5	5	7.5	10	Average	Deviation
Density, measured values [kg/m ³]	1324	1697	895	785	1978	1336	6.02%
Density, theoretical c used [kg/m ³]	1370	1740	894	767	2006	1355	7.57%
Density, theoretical R used [kg/m ³]	1208	1218	1250	1278	1231	1237	1.82%
Density, average c and R [kg/m ³]	-	-	-	-	-	1332	5.73%

In table 4.4 the speed of sound in glycerol is shown. The average value of the speed of sound is found and deviates less than 1% from the theoretical value. With these measured results the density of glycerol is calculated. The density is calculated in several ways to see the influence of the measured reflection coefficient or the measured speed of sound on the calculated density. In table 4.5 the density calculations with the measured values of table 4.4 deviate from the theoretical value but when averaged this deviation is no more than 6%. This is shown in the first row. The second row shows the density when the theoretical value for the speed of sound is used. It displays a value of 1355 kg/m³ and deviates 7.57%, whereas the third row shows the density when the theoretical value for the reflection coefficient is used and has a value of 1237 kg/m³ and deviates 1.82% from the actual value. From the density calculations with the different theoretical values, it can be deducted that the deviation in density calculation is mainly caused by reflection coefficient. In the fourth row the density is calculated with the average values of the reflection coefficient and the speed of sound. Its value is 1332 kg/m³ and deviates 5.73% from the theoretical value. In the next part the attenuation coefficient is calculated. With this coefficient, and the calculated values density and speed of sound in glycerol, the viscosity can be calculated.

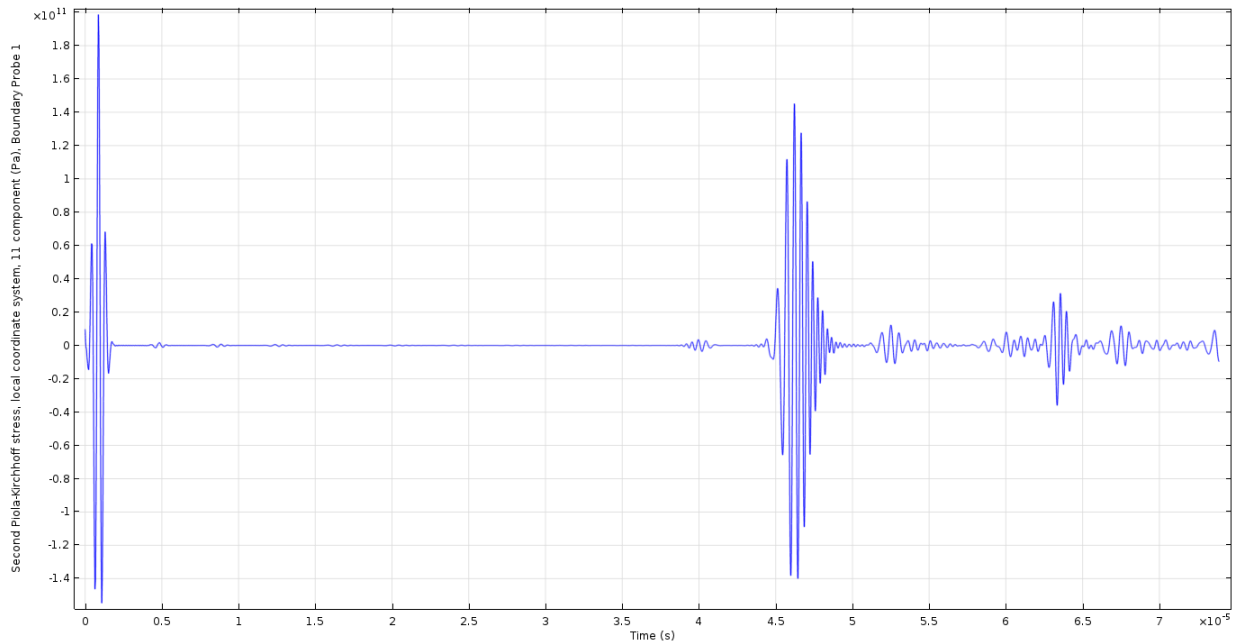


Figure 4.11: Plot of a pulse measurement top probe of a tapered copper rod with length 100 mm, width 17 mm at 0 mm decreased fluid depth of glycerol with a tapering angle of 1.25°. Eight mesh elements per wavelength used.

4.5.2 Attenuation measurement and viscosity calculation

Only the results of glycerol are used for the measurement of the attenuation coefficient. The initial depth of the fluid is 17 mm. The fluid depth will be reduced by 2.5 mm until a fluid depth of 7 mm is reached. One simulation per depth is done and eight mesh elements per wavelength are used. In order to find the attenuation coefficient the intensities of the transmitted waves are measured and these values are displayed in table 4.6.

The attenuation coefficient can be calculated using equation 2.21. This calculation depends on the difference of the fluid depths. Therefore calculations are done to find the attenuation coefficients at different fluid depth difference. The calculations are done at 2.5 mm, 5 mm, 7.5 mm and 10 mm depth differences and are shown in table 4.7. To reduce the fluctuations the average value of the attenuation coefficient is calculated. It has the value 17.08 1/m and deviates 52.33% from the theoretical value. This deviation is significant larger than the deviations of previously calculated properties. An explanation for this deviation is the fact that the transmitted wave and trailing echoes come back at the receiver at approximately the same time interval. This means that when measuring this signal, no distinction can be made between desired signal and noise. Also, because of these disturbance in this signal it is difficult to make a distinction between where the desired signal begins and ends. Thus some kind of computational error with this set up is inevitable.

The calculated viscosity is shown in table 4.8. The viscosity is calculated using equation 2.21 and the calculated average values of density, speed of sound of glycerol and the attenuation coefficient. The calculated value of the viscosity is 1.58 Pa s and deviates 66.36% from the theoretical value. This deviation is caused by the deviations of before mentioned average values of which the attenuation deviation contributes the most. To improve the viscosity measurement method it is imperative to improve the measurement of the attenuation coefficient. This can be accomplished by an optimal tapering angle to reduce the trailing echoes as much as possible. When this is optimised, measurements of the intensities of the trailing echoes have to be done in order to filter out this noise of the measurements of the intensities of the transmitted waves. This should improve the measurement method

Table 4.6: Measured intensities of transmitted waves in glycerol at different depths.

Decreasing fluid depth [mm]	0	2.5	5	7.5	10
Intensity of transmitted wave [10^{12} Pa]	1.56	1.73	2.09	2.11	1.84

Table 4.7: Averaged attenuation coefficients at different depth differences and their average. The theoretical value of the attenuation coefficient is 11.21.

Depth difference [mm]	2.5	5	7.5	10	Average
Average attenuation coefficient [1/m]	22.01	12.16	12.16	8.39	17.08
Deviation from theoretical value	96.26%	8.40%	8.40%	25.14%	52.33%

Table 4.8: Result of the viscosity calculation. The average values and $\omega = (2 * \pi * f)$ with $f = 2$ MHz are used in equation 2.21 to calculate the viscosity. The theoretical value of the viscosity is 0.95 [Pa s]

Average density [kg/m ³]	1332
Average speed of sound [m/s]	1939
Average attenuation [1/m]	17.08
Viscosity [Pa s]	1.58
Deviation from theoretical value	66.36%

Chapter 5

Conclusion and recommendation

The goal of this research was to calculate the density and viscosity of glycerol using acoustic waves in a copper waveguide. The measurements were done with a 2D simulation model created in COMSOL. In order to calculate the density of glycerol, the reflection coefficient and the speed of sound in glycerol were measured. The measured value of the reflection coefficient was 0.882 which deviates about 0.9% from the theoretical value 0.890. The calculated value of the speed of sound was 1939.1 m/s which deviates about 0.99% from 1920 m/s. The density of glycerol was therefore calculated as 1332 kg/m³. This result deviates 5.73% from the actual density of glycerol, which is 1260 kg/m³. To calculate the viscosity of glycerol, the reflection coefficient, the speed of sound and the attenuation coefficient of the fluid are necessary. The attenuation coefficient is calculated by measuring the intensities of the transmitted pulses in the fluid, which are received later than the reflected pulses from the solid-liquid interface. The calculated value of the attenuation coefficient is 17.08 1/m and this result deviates 52.33% from the theoretical value of 11.21 1/m. With this attenuation and the previous results, the viscosity of glycerol was calculated. The calculated viscosity is 1.58 Pa s that deviates 66.36% from the actual value 0.95 Pa s.

The deviation from the theoretical value of density is mainly inflicted by the deviation of the reflection coefficient, but still within limits. The deviation of viscosity is caused by the attenuation coefficient. This deviation is larger than the previously calculated values. The reason for such deviation is that the received wave from glycerol and the trailing echoes come back at the receiver at approximately the same time interval. Therefore no good distinction can be made between desired signal and noise. Also, because of these disturbance in this signal it is difficult to make a distinction between where the desired signal begins and ends.

To improve the determination of the density and viscosity, it is necessary to eliminate the trailing echoes as much as possible. Also, a minimum of two immersion depths has to be chosen at which the trailing echoes are minimised. It is important to collect as much data as possible for calculation of the attenuation coefficient, thus more simulations have to be done. Lastly, instead of using acoustic waves in a waveguide it is possible to use surface waves for the determination of density and viscosity. With this method, only the first peak has to be measured and the attenuation is higher [14]. This reduces the computation time and should be investigated in further research.

If the determination of the density and viscosity are optimised, eventually predictions can be made for critical information of the MSFR. This will contribute to the final goal of this project to deliver experimental proof of the safety and sustainability features of the MSFR.

Appendix A

Parameters

Name	Expression	Value	Description
Lrod	-	0.15 <i>m</i>	Length of rod
Hrod	-	0.025 <i>m</i>	Width of rod
c-long	-	4600 <i>m/s</i>	Longitudinal wave speed in copper
c-trans	-	2270 <i>m/s</i>	Transverse wave speed in copper
c-fluid-water	-	1480 <i>m/s</i>	Speed of sound in water
Freq	-	$2 * 10^6$ <i>Hz</i>	Frequency of pulse
lambda-c-long	c-long/Freq	0.0023 <i>m</i>	Wave length of longitudinal wave
lambda-c-trans	c-trans/Freq	0.001135 <i>m</i>	Wave length of transversal wave
lambda-fluid	c-fluid-water/Freq	$7.4 * 10^{-4}$ <i>m</i>	Wave length of wave in fluid
Nq	-	0.2	Scaling element for finer time step size
time step	Nq*lambda-c-long/c-long	$1 * 10^{-7}$ <i>s</i>	Distance between measurement points
tpulse	1/Freq	$5 * 10^{-7}$ <i>s</i>	Duration of one pulse
NP	-	3.5	Width of pulse
w	-	$5 * 10^{-10}$	Scaling factor for pulse
timelimit	4*(Lrod/c-long)	$1.3043 * 10^{-4}$ <i>s</i>	Time for two pulse measurements
N	-	8	Mesh elements per wave length
K1	Lrod*N/lambda-c-long	521.74	Mesh y-direction
K2	Hrod*N/lambda-c-trans	176.21	Mesh x-direction
ysub	-	0 <i>mm</i>	level of immersion

Table A.1: Calculated density values of glycerol for different chosen reflection coefficients and speed of sound in glycerol. The theoretical value of the density of glycerol is 1260 [kg/m³]

Depth of fluid [mm]	0	2.5	5	7.5	10	Average
Density, measured values [kg/m ³]	1324	1697	895	785	1978	1336
Deviation from theoretical value	5.11%	34.68%	28.95%	37.73%	57.01%	6.02%
Density, theoretical c used [kg/m ³]	1370	1740	894	767	2006	1355
Deviation from theoretical value	8.70%	38.08%	29.04%	39.15%	59.22%	7.57%
Density, theoretical R used [kg/m ³]	1208	1218	1250	1278	1231	1237
Deviation from theoretical value	4.16%	3.32%	0.76%	1.42%	2.26%	1.82%
Density, average c and R [kg/m ³]	-	-	-	-	-	1332
Deviation from theoretical value	-	-	-	-	-	5.73%

Bibliography

- [1] World-nuclear.org. (2017). Generation IV Nuclear Reactors: WNA - World Nuclear Association. [online] Available at: <http://www.world-nuclear.org/information-library/nuclear-fuel-cycle/nuclear-power-reactors/generation-iv-nuclear-reactors.aspx> [Accessed 26 Sep. 2017].
- [2] SAMOFAR. (2017). Project - SAMOFAR. [online] Available at: <http://samofar.eu/project/> [Accessed 26 Sep. 2017].
- [3] S. Mastromarino, Determination of Thermodynamic properties of Molten Salt, periodic report, University of Technology Delft (2016)
- [4] Serp, J., Allibert, M., Beneš, O., Delpéch, S., Feynberg, O., Ghetta, V., Heuer, D., Holcomb, D., Ignatiev, V., Kloosterman, J., Luzzi, L., Merle-Lucotte, E., Uhlíř, J., Yoshioka, R. and Zhimin, D. (2017). The molten salt reactor (MSR) in generation IV: Overview and perspectives.
- [5] M. Allibert, D. Gérardin, D. Heuer, E. Huffer, A. Laureau, E. Merle, S. Beils, A. Cammi, B. Carluéc, S. Delpéch, A. Gerber, E. Girardi, J. Krepel, D. Lathouwers, D. Lecarpentier, S. Lorenzi, L. Luzzi, S. Pומרouly, M. Ricotti, and V. Tiberi. Description of initial reference design and identification of safety aspects. Work Package 1, Deliverable D1.1, SAMOFAR (Safety Assessment of the MOLten Salt FAsT Reactor) European project, Contract number: 661891, 2016.
- [6] Panametrics Ultrasonic Transducers. (2017). [PDF] Athens: OLYMPUS, p.6. Available at: <http://www.envirocoustics.gr/products/ultrasonic/pdf/Panametrics-UT-Transducers.pdf> [Accessed 28 Sep. 2017].
- [7] H.A.J. Froeling, Causes of spurious echoes by ultrasonic wave simulation, bsc. thesis, University of Technology Delft (2017)
- [8] T. Ihara, N. Tsuzuki, and H. Kikura. Development of the ultrasonic buffer rod for the molten glass measurement. *Progress in Nuclear Energy*, 82:176–183, 2015.
- [9] T.S. Oud, Elastic wave simulation for buffer rod tapering, bsc. thesis, University of Technology Delft (2017)
- [10] COMSOL. version 5.2a. 2015
- [11] W.C. Elmore and M.A. Heald. McGraw-Hill Book company, 1969.
- [12] E. Flores-Mendez, M. Carbajal-Romero, N. Flores-Guzman, R. Sanchez-Martinez, A. Rodriguez-Castellanos. Rayleigh's, Stoneley's, and Scholte's Interface Waves in Elastic Models Using a Boundary Element Method. Instituto Politecnico Nacional (2012)

- [13] Phys. Today 55(3), 42 (2002); doi: 10.1063/1.1472393
- [14] F. B. Cegla, P. Cawley, and M. J. S. Lowe. Material property measurement using the quasi-Scholte mode—A waveguide sensor. Imperial College London (2004)
- [15] Rose, J. (2014). Ultrasonic guided waves in solid media. New York: Cambridge University Press.
- [16] F. B. Cegla. Ultrasonic waveguide sensors for fluid characterisation and remote sensing. Imperial College London (2006)
- [17] P. Roux, B. Roman, and M. Fink. Time-reversal in an ultrasonic waveguide. Applied Physics Letters, 70:1811–1813, 1997. Ashcroft, N., Mermin, D. (1976). Solid stat physics. New York: Rinehart and Winston.
- [18] Hisham, Comsol convergence tips. [online]
Available at: <https://community.cmc.ca/docs/DOC-1453> [Accessed at 22 Oct. 2017].
- [19] D. Andrews, Modelling of ultrasonic transducers and ultrasonic wave using finite elements, 2014 COMSOL Conference Cambridge
- [20] MATLAB. version (R2016b). The MathWorks Inc., Natick, Massachusetts, 2017